García Ivars, J.; Alcaina Miranda, MI.; Iborra Clar, MI.; Mendoza Roca, JA.; Pastor Alcañiz, L. (2014). Enhancement in hydrophilicity of different polymer phase-inversion ultrafiltration membranes by introducing PEG/Al2O3 nanoparticles. Separation and Purification Technology. 128:45-57. doi:10.1016/j.seppur.2014.03.012.

Enhancement in hydrophilicity of different polymer phase-inversion ultrafiltration membranes by introducing PEG/Al_2O_3 nanoparticles

Jorge Garcia-Ivars*[1], Maria-Isabel Alcaina-Miranda[1,2], Maria-Isabel Iborra-Clar[1,2], José-Antonio Mendoza-Roca[1,2], Laura Pastor-Alcañiz[3]

[1]Research Institute for Industrial, Radiophysical and Environmental Safety (ISIRYM), Universitat Politècnica de València, C/Camino de Vera s/n, 46022 Valencia, Spain

[2]Department of Chemical and Nuclear Engineering, Universitat Politècnica de València, C/Camino de Vera s/n, 46022 Valencia, Spain

[3]Depuración de Aguas de Mediterráneo, Avda. Benjamin Franklin, 21, Parque Tecnológico 46980 Paterna, Spain

Tel. +34 9637879633

Fax. +34 963877639

Correspondence to: Jorge Garcia-Ivars (E-mail: *jorgariv@posgrado.upv.es*)

ABSTRACT

The influence of the modification by additives in the characteristics of several ultrafiltration polymeric membranes was studied. Three asymmetric membranes with similar pore size (molecular weight cut-off (MWCO) of around 30 kDa) but different materials and pore microstructures – polysulfone, polyethersulfone and polyetherimide – were used. Effects of two different hydrophilic additives on membrane structure and the resulting performance were compared to determine the material with the best antifouling properties. Polyethyleneglycol (PEG) and alumina (Al_2O_3) were employed as additives in the phase-inversion method, N,N-Dimethylacetamide and deionized water were used as solvent and coagulant, respectively. Membranes were characterized in terms of hydraulic permeability, membrane resistance, MWCO profile and

hydrophilicity (by membrane porosity and contact angle). The cross-sectional and membrane surface were also examined by microscopic techniques. Membrane antifouling properties were analysed by the experimental study of fouling/rinsing cycles using feed solutions of PEG of 35 kDa. Permeation and morphological studies showed that the addition of PEG/Al_2O_3 results in formation of a hydrophilic finger-like structure with macrovoids, whereas the addition of Al_2O_3 results in the formation of a hydrophilic structure with a dense top layer with Al_2O_3 nanoparticles and a porous sponge-like sublayer. Furthermore, polyethersulfone/PEG/Al_2O_3 membranes displayed superior antifouling properties and desirable ultrafiltration performance.

KEYWORDS membrane preparation; hydrophilicity; phase-inversion method; alumina; polyethyleneglycol.

1. INTRODUCTION

Ultrafiltration (UF) is a pressure-driven membrane separation process using membranes with pore sizes between 0.1 and 0.001 μm. This technique is widely used for separating macromolecules, proteins, colloids, and suspended particles from different solutions in several industrial fields, such as water production, chemicals processing, food processing, biotechnology, and water and wastewater treatment [1,2]. Due to the growing application of UF process, efforts to improve UF process performance are gaining more and more importance.

Commercial UF membranes are prepared using several polymers like cellulose acetate (CA), polyacrylonitrile (PAN), polyetherimide (PEI), polyethersulfone (PES), polyethylene (PE), polypropylene (PP), polysulfone (PS) and polyvinylidene fluoride

(PVDF), and among them PS and PES are the most common polymers used in membrane preparation because their mechanical strength and physicochemical characteristics for UF applications [3]. Unfortunately, the inherent hydrophobic nature of PS and PES membranes makes them susceptible to be contaminated, which can lead to a decline of permeability properties and membrane lifetime [4,5].

Therefore, the contamination of the membrane, known as membrane fouling, is an important problem in UF. Membrane fouling depends on membrane surface characteristics such as morphology, pore size, porosity, and hydrophilicity [6]. During an UF process, the initial blockage of the membrane pores results in a rapid flux decline. After that, the accumulation of the retained macromolecules on the membrane surface leads to a gradual flux decline [7,8]. To avoid this problem, the composition of the membrane can be modified in order to obtain a more hydrophilic material. So, the increase of the hydrophilicity of the membrane surface and pore surfaces can remarkably reduce membrane fouling [9,10].

Many researchers have studied the modification of the membrane surface properties [6,8,11,12] in terms of hydrophilicity, pore size, porosity and surface charge, which has several advantages as the inhibition of the foulants adsorption and deposition, and hence an increase in the permeate flux and a decrease in membrane fouling. However these modifications change the internal structure of the membrane, making irreversible changes in pore size distribution of the membranes. Therefore recent studies are focused on the addition of organic and inorganic nanoparticles within the membrane matrix [5].

The use of organic or inorganic nanoparticles as additives in membranes to decrease its hydrophobicity is extensively reported. The presence of nanoparticles in the membrane matrix improves the thermal stability, strength and stiffness, permeability, hydrophilicity, flux recovery and antifouling property of the membrane [5,13-15]. Also the addition could control the membrane surface properties and prevent the macrovoids formation [9,16,17]. However, uniform and homogeneous dispersion of the additives in the casting solution is very difficult due to the high viscosity of the casting solution and the ease of the nanoparticles to agglomerate [5,18]. This agglomeration could result in the decrease of pure water flux (PWF) because of the blockage of the membrane pores is caused by the high content of nanoparticles in the membrane matrix [13].

One of the most common methods to prepare membranes is the phase-inversion process. The phase-inversion method induced by immersion precipitation has been widely used for preparing asymmetric polymeric membranes. This is a useful method to introduce nanoparticles as additives in the membrane matrix [19,20]. In this process, the membrane preparation is influenced by many factors, including the concentration and state of the polymer and solvent, the composition of the non-solvent in the coagulation bath, and the role and concentration of the additive. Several studies [21-25] had demonstrated that the addition of organic/inorganic nanoparticles in the casting solution could enhance the phase-inversion process, adjusting the membrane properties. Additives modify the membrane surface and structure by changing the kinetics and thermodynamics of the formation process. Ochoa et al. (2003) prepared PVDF with polymethyl methacrylate (PMMA) membranes with different degrees of hydrophilicity, obtaining the appearance of macrovoids in the porous substructure without any modification of the selective surface structure and high hydrophilic character when

PMMA concentration increases [26]. Yan et al. (2005) prepared PVDF membranes modified by nano-sized alumina (Al_2O_3), improving the surface hydrophilicity, pure water flux (PWF), flux recovery and then antifouling character in comparison with unmodified membranes [27]. Chakrabarty et al. (2008) modified PS membranes with the addition of polyethyleneglycol (PEG) of different molecular weight, causing the increase in the PWF and BSA rejection when the molecular weight of PEG increases [28]. Saljoughi et al. (2010) studied the effect of coagulation bath temperature (CBT) and different PEG concentrations in prepared CA with PEG and 1-methyl-2-pyrrolidone, resulting in the increase of porosity and permeability with the presence of low molecular weight PEG and the increase of thermal/chemical stability of the prepared membranes with the decline of CBT [20].

In the present work, alumina (Al_2O_3) and PEG of molecular weight 400 Da (PEG 400) are used as additives to obtain a hydrophilic polymeric membrane having a molecular weight cut-off of around 30 kDa. Al_2O_3 is one of the most stable inorganic materials, inexpensive, highly abrasive, resistant and non-toxic (even in form of nanoparticles). Previous studies [27,29,30] have demonstrated that the use of Al_2O_3 nanoparticles in UF membranes is of interest. PEG has been extensively used as additive to enhance the membrane preparation. Shieh et al. (2001) showed that PEG is used to improve membrane selectivity as well as a pore forming agent due to its hydrophilic nature [31]. Liu et al. (2003) reported that PEG 400 can be used as polymeric additive to improve the hydrophilicity and to prevent the macrovoid formation when PEG 400 is added in appropriate amounts [16].

This research aimed to study the influence of the combination of two compounds with different nature, an organic additive (PEG 400) with an inorganic additive (Al_2O_3), on the preparation of several UF polymeric membranes with different chemical and physical properties to improve their hydrophilicity. Until now, no papers dealing with the combination of both types of additives for membrane modification by phase inversion method have been published. The effect of addition of PEG 400 and nano-sized Al_2O_3 at different concentrations in casting solution on morphology, permeability properties and on the hydrophilicity of the membranes were investigated. Morphology and composition of each membrane were analysed by scanning electron microscope (SEM) and energy dispersive X-ray (EDX). Membrane hydrophilicity was also determined using contact angle measurements. The performances of the prepared membranes were tested by water permeation and different molecular weights of PEG rejection.

2. EXPERIMENTAL

2.1 Materials

Polyethersulfone (PES, Ultrason E 6020 P, M_W = 51000 Da) and polysulfone (PS, Ultrason S 2010, M_W = 42000 Da) were purchased from BASF Co. (Germany). Polyetherimide (PEI, Ultem 1010, M_W = 48000 Da) was donated by General Electric (United States). These polymers were independently used as base polymer in the different membrane casting solutions. The nonwoven support was commercial grade Viledon FO 2431 from Freudenberg (Germany). The solvent N,N-Dimethylacetamide (DMA) was selected in the current study because it is widely accepted as a good solvent for many polymers [22, 32, 33]. Aluminium oxide (Al_2O_3) in gamma phase with primary particle size of 13 nm and a surface area of 90 m^2/g (Sigma Aldrich, Germany)

was used as an inorganic hydrophilic additive. Also, polyethyleneglycols with different molecular weight of 400, 10000, 20000 and 35000 Da were provided by Sigma Aldrich (Germany). The additives (Al_2O_3 and PEG400) were specifically selected to study the effects of the organic/inorganic nature on the membrane performance. Deionized water was used throughout this study.

2.2. Membrane preparation

Phase-inversion method by immersion precipitation was applied for preparing asymmetric ultrafiltration membranes. Homogeneous solutions were prepared by dissolving PEG in DMA in the presence of Al_2O_3 under vigorous and constant mechanical stirring with a vortex mixer at a room-temperature, in which PEG was rapidly dissolved and Al_2O_3 nanoparticles were dispersed. After that, a predetermined amount of each polymer was added with continuous stirring for at least 48 h until the solution was completely dissolved and homogeneous. The effect of polymer concentration was studied by preparing casting solutions consisting of 15 and 20 wt%. According to previous studies about modification of organic membranes, these polymer compositions were selected to prepare membranes [10]. When polymer was completely dissolved, Al_2O_3 was well-dispersed and also entrapped into the polymer solution matrix due to the high viscosity of the polymer solution. Then, the resultant polymer solutions were centrifuged at 1500 rpm during 2 min, and placed in a desiccator to keep intact their characteristics and release all of the bubbles. Membranes were cast with a 75 μm casting knife onto nonwoven supports by using a film applicator at room-temperature. After that, membranes were immediately immersed in a coagulation bath of deionized water at 18 ºC for 48 h to not allow a preceding dry phase-inversion in the atmosphere [34] and to remove the remaining solvent from the membrane structure

175 [35]. After complete the coagulation process, the prepared UF membranes were stored
176 in deionized water until use.
177
178 *2.3. Characterization of membranes*
179 All the membranes prepared were characterized in terms of pure water flux, hydraulic
180 permeability and membrane resistance, fouling/rinsing experiments, MWCO
181 determination, porosity, equilibrium water content, contact angle, and morphological
182 studies as follows.
183
184 *2.3.1 Hydraulic permeability*
185 UF experimental set up used in this part of the study is shown schematically in Fig. 1.
186 This system consisted of a temperature-controlled feed tank (1) with 20 L in volume, a
187 centrifugal pump (4), a pre-filter (3) with a nominal pore size of 100 μm, and two UF
188 membranes inside a RAYFLOW X100 cross-flow membrane module supplied by
189 TECHSEP (6), where the effective membrane area was 100 cm^2. Feed solution stream
190 crosses the membrane module, dividing it into two different streams, permeate and
191 concentrate. Both streams return to the feed tank. The required transmembrane pressure
192 is obtained by two manometers (0-600 kPa), placed at the inlet (5) and outlet (7) of the
193 membrane module, which are controlled by two throttling valves (2 and 8). Also, a flow
194 meter (9) is placed at the concentrate outlet and is used to measure cross-flow rate.
195
196 Water permeation properties of asymmetric polymeric membranes were tested using the
197 above-mentioned cross-flow filtration system. Initially, membranes were compacted at
198 100 kPa of transmembrane pressure (ΔP) for 30 minutes. Then, hydraulic permeability
199 experiments were carried out with deionized water. Flux was measured at different

transmembrane pressures ranging from 100 to 300 kPa at a constant flow rate of 300 L h^{-1} and at room-temperature conditions. J_W (L m^{-2} h^{-1}) was evaluated by the expression,

$$J_W = \frac{V}{A_m \cdot t} \quad \text{Eq. (1)}$$

where V is the total volume permeated (m^3) during the experimental time interval t (h) and A_m is the effective surface area of the membrane (m^2).

Hydraulic permeability (P_h) was obtained from the slope of the plot of J_W and ΔP and was calculated by

$$P_h = \frac{J_W}{\Delta P} \quad \text{Eq. (2)}$$

Membrane intrinsic resistance or membrane resistance (R_m) was calculated according to Darcy's law (Eq. (3)):

$$R_m = \frac{\Delta P}{\mu \cdot J_W} \quad \text{Eq. (3)}$$

where μ is the water viscosity (Pa s).

2.3.2 Molecular weight cut-off determination

Molecular weight cut-off (MWCO) of the membranes was determined using 1 g L^{-1} aqueous solutions of PEG with different molecular weights from 10 to 35 kDa. PEG solutions were prepared individually using deionized water and used as a standard for rejection studies. Experiments were carried out at a constant cross-flow velocity (2.08 m s^{-1}), 25 ºC, and ΔP ranging from 50 to 400 kPa in the same above-mentioned ultrafiltration set up. PEG concentrations were analysed using a high-precision Atago

Refractometer (Atago RX-5000) at 20 °C within an accuracy of ± 0.00004 units. Rejection (R) was calculated by Eq. (4):

$$R(\%) = \left(1 - \frac{C_p}{C_f}\right) \cdot 100 \qquad \text{Eq. (4)}$$

where C_p is the concentration of PEG in permeate and C_f is the concentration of PEG in the feed solution.

The smallest molecular weight that is rejected by 90% is taken as the MWCO of the membrane [36]. Membranes with higher rejection and lower MWCO were selected for following studies.

2.3.3 Fouling experiments

After obtaining the MWCO and the hydraulic permeability, selected membranes were subjected to a series of fouling experiments with hydraulic cleaning (rinsing). Firstly, water flux tests were performed for each selected membrane at 200 kPa at a constant flow rate of 300 L h^{-1} during 30 min. Then, a solution of PEG of 35 kDa with a concentration of 5 g L^{-1} was used as a feed solution in fouling studies. PEG has been extensively used as a standard macromolecule in different UF experiments to study fouling models and hydrophilicity properties [2, 37]. The permeate flux during PEG ultrafiltration J_f (L m^{-2} h^{-1}) was measured by weighing permeate versus time at 200 kPa for 2 h. After filtration of PEG solution, fouled membranes were washed with deionized water for 30 min, measuring the water flux of the tested membranes. These experiments were repeated three times. In order to evaluate the fouling-resistant ability of the prepared membranes, normalized flux ratio (*NFR*) was calculated by the following expression.

$$NFR(\%) = \left(\frac{J_{f2}}{J_{f1}} \right) \cdot 100 \qquad \text{Eq. (5)}$$

where J_{f2} is the flux of the membranes after the fouling process (2 h) and J_{f1} is the flux of the membranes obtained at the beginning of each fouling cycle.

Generally, higher *NFR* values (next to 1) indicate better antifouling property of the membrane.

2.3.4 Surface hydrophilicity

Water contact angle on membrane surfaces was measured using an optical instrument (Dataphysics OCA20, Germany) for predicting hydrophilicity. Before water contact angle measurements, membrane samples were dried and stored in a vacuum desiccator during 24 h. Three microlitres of water were dropped on the dried flat membrane surface from a microsyringe with a stainless steel needle at room-temperature conditions. Deionized water was used as the probe liquid in all the measurements. Contact angle values were averaged from ten random locations for each membrane. If membranes are hydrophilic, the angle stays lower than 90º [38].

In addition, two parameters were studied to determine the degree of hydrophobicity of a membrane: equilibrium water content (*EWC*) and membrane porosity (ε). Both parameters play an important role on permeation and separation [28]. After the membrane was equilibrated in water, the volume occupied by water and the volume of the membrane in wet state were determined. Membranes were mopped with a tissue paper to remove the water layer retained on the membrane surface, obtaining the wet membrane samples. These samples were weighed in wet state. After that, wet samples

were dried by putting in a vacuum oven for 24 h at 50 ºC and then they were weighed in dry state. Membrane porosity was defined as the volume of the pores divided by the total volume of the membrane. Membrane porosity was obtained using the following equation,

$$\varepsilon(\%) = \frac{\frac{(W_W - W_D)}{\rho_W}}{\frac{(W_W - W_D)}{\rho_W} + \frac{W_D}{\rho_p}} \cdot 100 \qquad \text{Eq. (6)}$$

where W_W is the weight of wet membranes (g), W_D is the weight of dry membranes (g), ρ_W is the density of pure water at operating conditions (g cm^{-3}), and ρ_p is the density of the polymer (g cm^{-3}) [23].

EWC was estimated by

$$EWC(\%) = \frac{W_W - W_D}{W_W} \cdot 100 \qquad \text{Eq. (7)}$$

Values of membrane porosity and EWC were averaged from five different samples of the same prepared membrane to minimize the error of the weighing measurements.

2.3.5 Average pore radius

Membrane pore size is a useful parameter to evaluate the membrane performance. Membrane average pore radius (r_m) is regarded as an estimation of true pore size and it represents the average pore size along the membrane thickness (ζ). This parameter was determined by water filtration velocity method under constant transmembrane pressure (300 kPa) and it could be calculated by the Guerout-Elford-Ferry equation [23,35],

$$r_m = \sqrt{\frac{(2.9 - 1.75 \cdot \varepsilon) \cdot (8 \cdot \mu \cdot \zeta \cdot Q_W)}{\varepsilon \cdot A_m \cdot \Delta P}} \qquad \text{Eq. (8)}$$

where μ is the water viscosity (Pa s), Q_W is the water flow (m^3 s^{-1}) and ΔP is the transmembrane pressure (MPa).

2.3.6 Morphological studies

A multimode atomic force microscopy (VEECO Instruments (USA)) was also used to characterize the surface of all membranes. All AFM images were taken in ambient air in tapping mode and were obtained over different areas of each membrane sample. The tapping mode is ideal for the study of relatively soft samples such as grafted polymers [39]. Roughness values were obtained from 5 μm x 5 μm samples and considering the average of five areas of 1 μm x 1 μm. The average roughness (S_a) and the root mean square roughness (S_q) are expressed as follows [40]:

$$S_a = \frac{1}{N}\sum_{i=0}^{N}\left|Z_i - Z_{avg}\right| \quad \text{Eq. (9)}$$

$$S_q = \sqrt{\frac{1}{N}\sum_{i=0}^{N}\left|Z_i - Z_{avg}\right|^2} \quad \text{Eq. (10)}$$

where Z_{avg} is the average of the Z values within the given area, Z_i is the current Z value measured and N is the number of points within the given area.

The cross-sectional morphologies of the prepared membranes were observed by scanning electron microscopy (SEM). For this purpose, membranes were frozen in liquid nitrogen, and then broken and sputtered with a thin conductive layer of carbon, prior to SEM analysis. During SEM observation, energy dispersive X-ray spectroscopy (EDX) analysis was performed to reveal the real composition of a certain part of the membrane. In this research, both analyses were carried out with a scanning electron microscope and its adjunct EDX analyser (JEOL JSM6300 scanning microscope,

315 Japan). Each reported element composition value was expressed by the average of three
316 measurements for each sample.
317
318 ## 3. RESULTS AND DISCUSSION
319 ### *3.1 Hydraulic characterization*
320 UF membranes were prepared using different polymers and additives. Table 1 shows
321 the effect of different polymer concentrations as well as the incorporation of different
322 PEG/Al_2O_3 concentrations on the membrane hydraulic permeability and the membrane
323 resistance. The hydraulic permeability of membranes prepared with 20 wt% polymer
324 concentration was lower than 15 wt%, because an increase in polymer concentration in
325 the casting solution leads to a more thermodynamically stable membrane with denser
326 structure and less macrovoids [41]. As a consequence, hydraulic permeability declines
327 but membrane resistance increases. Lohokare et al. (2011) had investigated the
328 optimization of membrane preparation parameters on membrane morphology and
329 separation performance (including the effect of polymer concentration and additive).
330 These researchers showed that an increase in polymer concentration at constant solvent
331 ratio produced higher solution viscosities and selectivity but generally lower membrane
332 pore size. The aforementioned authors demonstrated that there was an optimal
333 composition (20.5 wt% PAN concentration) up to which these effects had been
334 achieved. A further increase in polymer concentration caused an increase in membrane
335 pore size because a very high viscosity resulted in a delayed gelation [42].
336
337 As shown in Table 1, addition of Al_2O_3 caused an increase in hydraulic permeability
338 and a decrease in membrane resistance. Generally, incorporation of additives in the
339 casting solution increases the water permeation rate. Water flux of the modified

membranes should be higher than water flux of the unmodified membranes due to the improvement of membrane hydrophilicity [5,27]. But this increase depends on the nature of the additive as well as the homogeneity of its dispersion in the base polymer. For PEI membranes, incorporation of additives in the polymer matrix caused a significant increase in hydraulic permeability in contrast to PES and PS membranes; especially in membranes with low polymer concentration. In this case, hydraulic permeability showed higher differences between unmodified and modified membranes. This phenomenon could be due to the hydrophilicity nature of PEI.

According to Maximous et al. (2009), membrane permeability increased as the nanoparticles concentration in the casting solution increased. During the phase-inversion process, these authors demonstrated that penetration velocity of water into nascent membrane increased with Al_2O_3 concentration due to the higher affinity of Al_2O_3 for water than base polymer (PES in their research). In addition, the interaction between polymer and solvent molecules decreased due to the hindrance of nanoparticles, which causes an easier diffusion of these solvent molecules from polymer matrix. Therefore, porosity and pore size of modified membranes with Al_2O_3 were slightly higher than those of unmodified membranes [41,43]. However, higher contents of nanoparticles could negatively affect the membrane permeability due to agglomerations of the inorganic nano-sized Al_2O_3 particles on the membrane matrix during the membrane preparation, decreasing their dispersion in the polymeric membrane. These agglomerated nanoparticles may clog some pores causing a decline in the water flux [44]. These agglomerations may be caused by attractive Van der Waals forces, which could give rise to defects and heterogeneities in membrane morphology [45]. Hydraulic permeability also increased with the addition of PEG/Al_2O_3 principally

365 due to the pore forming character of the PEG 400 [31,46]. As an example, for
366 membranes prepared using 20 wt% PES, hydraulic permeability increased from 2.352 L
367 m^{-2} h^{-1} kPa^{-1} to 5.146 L m^{-2} h^{-1} kPa^{-1}. Consequently, the combined addition of
368 PEG/Al_2O_3 resulted in a high PWF, and hence in an increase in hydraulic permeability
369 and a low membrane resistance.
370
371 *3.2 Molecular weight cut-off determination*
372 To determine the MWCO of the prepared membranes, different molecular weights of
373 PEG (10, 20 and 35 kDa) were used as feed solutions. Fig. 2 presents the MWCO of
374 the prepared membranes in absence and presence of PEG and Al_2O_3. The trend
375 observed by the different cut-off curves is similar to those obtained in the study of PEGs
376 retention and MWCO determination by several other authors [17, 47]. At the same
377 conditions, all the membranes prepared had a MWCO about 20 and 35 kDa, except all
378 the PEI membranes and PS membrane modified by Al_2O_3. These membranes showed a
379 higher MWCO than 35 kDa because solute rejection was lower than 90%. For such
380 membranes, the modification with nanoparticles increased the porosity and MWCO as
381 occurred with other additives such as TiO_2 and PVP studied by other authors [13,48]. In
382 addition, no significantly difference existed between unmodified membranes and
383 membranes prepared with PEG/Al_2O_3 as additive in PEG rejection. This phenomenon
384 can be explained if the separately effect of each additive is studied. When PEG
385 concentration increased, macrovoids formation and membrane porosity increased and
386 therefore, high PWF values and lower PEG rejection were obtained [17,20]. However,
387 increase in Al_2O_3 content could reduce membrane MWCO due to the aggregation
388 phenomenon of Al_2O_3 nanoparticles explained before (see Section 3.1). Thus,
389 modification with Al_2O_3 resulted in high values of solute rejection (see Fig. 2)

compared to the other membranes tested, therefore it is clearly shown that the PES membranes showed better performance when Al_2O_3 is added.

Regarding the polymer concentration, the comparison among all the membranes with PEG of 35 kDa as feed solution showed that there was a slightly improvement in solute rejection when the polymer concentration was 20 wt% compared to membranes of 15 wt% of polymer concentration. As the polymer concentration increased, the number of polymer molecules increased in the membrane surface and then, the pore size and MWCO decreased. However, prepared membranes showed a similar performance when PEG of 10 and 20 kDa were used as feed. Therefore, PES membranes were selected for fouling experiments, morphological and hydrophilicity studies.

3.3 Fouling experiments

Fouling experiments were performed to investigate the antifouling properties of the PES membranes modified with additives in comparison to PES membranes without nanoparticles of PEG or Al_2O_3. Firstly, PWF was measured during 30 min and then, three cycles of fouling/rinsing experiments were carried out for a total filtration time of 450 min. Each fouling experiment was performed with PEG (of 35 kDa) solution with a concentration of 5 g L^{-1} during 2 h, while each rinsing experiment was performed with deionized water during 30 min.

Fig 3 shows the results obtained for membranes with high PES concentration (20 wt% PES). After all the fouling/rinsing experiments, PES7 exhibited the highest flux recoveries with a final flux value of 488.03 L m^{-2} h^{-1} (85.12% of the initial value), whereas water flux value of the unmodified PES membrane (PES5) declined to 306.71

L m^{-2} h^{-1} (77.67% of the initial value). This behaviour could be caused by the introduction of the hydrophilic PEG/Al_2O_3 nanoparticles in the active layer, which made solute fouling less severe. However, PES8 showed the highest flux decline, presenting a final water flux of 224.71 L m^{-2} h^{-1} (59.53% of the initial value). This flux decline may be due to the excessive PEG 400 content in the membrane, which formed a membrane porous structure because of the intensification of thermodynamic instability of the cast film [20]. As Liu et al. (2003) demonstrated, PEG is a great polymeric additive to enhance the polymer dope viscosity and pore interconnectivity, which leads to enhance membrane hydrophilicity; although this improvement occurs when PEG is added in appropriate amounts [16].

Furthermore, the permeate flux of PES6 and PES7 slightly increased with operation time during the second and the third period of PEG ultrafiltration. Such phenomenon was opposite to the traditional results for fouling ultrafiltration. These results could be caused by the inherent interactions between foulant (PEG of 35 kDa) and Al_2O_3 nanoparticles presented in the membrane top layer [36]. Shi et al. (2008) obtained a similar behaviour for tertiary amine-modified PES membranes using BSA (1 g L^{-1}) as feed solution [21].

Fig. 4 shows the evolution of the parameter normalized flux ratio (*NFR*) with filtration time (2 h), where fouling degree of the original membrane and modified membranes can be compared. PES7 presented the highest *NFR* value (85.88%), which indicates lower total flux loss and thus, less foulant adsorption or deposition on the surface and pore walls of the membrane [49]. Consequently, the combined effect of PEG/Al_2O_3 resulted in a higher resistance towards fouling and reduced the hydrophobic interaction between

foulants and membrane surface [36]. Nevertheless, PES8 showed a significant decline in the permeate flux to about 60% of the initial flux, because the excessive PEG 400 caused an increase in porosity, pore size and macrovoids formation [50]. Therefore, PES7 exhibited better antifouling properties in the dynamic fouling process than the unmodified membrane (PES5) and PES/Al_2O_3 membrane (PES6).

Fig 5 shows the results obtained for membranes with low PES concentration (15 wt% PES). The flux decline was the highest for PES4 with a value of 571.80 L m^{-2} h^{-1} (64% of the initial value), which corroborated the negative effect of the excessive PEG 400 content in the membrane. After all the fouling/rinsing experiments, flux values of the unmodified PES membrane (PES1) declined to 212.75 L m^{-2} h^{-1} (77% of the initial value). Similar flux reduction was observed for PES (up to 489.82 L m^{-2} h^{-1}, 75% of the initial value) and PES3 (909.22 L m^{-2} h^{-1}, 77% of the initial value), which could be attributed to the similar MWCO of these membranes.

However, the hydrophilic effect of PEG/Al_2O_3 is clearly shown in Fig. 6. At low PES concentration, PES1 presented the lowest flux values, which declined to about 64.18% of the initial flux in 2 h. During the same filtration time, PES/Al_2O_3 membrane (PES2) exhibited higher resistance towards fouling with a flux decline to about 80.14% of the initial flux. Similar behaviour was observed for PES3 membrane (membrane with low PEG 400 content) with a flux decline to about 79.56% of the initial flux value.

Therefore, these results showed that the incorporation of PEG/Al_2O_3 nanoparticles in PES membranes improved their antifouling properties, obtaining a low decline of their normalized flux and a high rinsing efficiency [9]. But, it should be noted that the

PEG/Al_2O_3 addition in PES membranes could negatively affect their antifouling properties when PEG 400 content was higher than 2 wt%.

3.4 Porosity, EWC and average pore radius

Membrane porosity and EWC are two important parameters for membrane characterization to determine indirectly the degree of hydrophilicity or hydrophobicity of a membrane. Both parameters are related to PWF and then, to hydraulic permeability [28]. Several authors demonstrated their application in the characterization of different asymmetric polymeric membranes, in which pores on the membrane surface as well as cavities in the porous sublayer are responsible for accommodating water molecules in the membrane [5,23,28]. Average pore radius (r_m) was also applied in studies in which asymmetric membrane porosity was evaluated [23]. Results are presented in Table 2.

Firstly, all the prepared membranes showed a good porosity with values between 69 to 87%, which could be due to the low polymer concentration in the casting solution and the low membrane thickness over the nonwoven support. It is observed that porosity, *EWC*, and average pore radius of all the membranes enhanced with addition of PEG 400 content. Feng et al. (2006) demonstrated that macromolecules distribution must be influenced as a result of the addition of PEG [51] and other researchers confirmed the forming pore character of the PEG [50,52]. Also, Saljoughi et al. (2010) demonstrated that the presence of PEG in membrane composition facilities macrovoid formation in the membrane sublayer as well as increases the thickness of the prepared membranes [20]. However, the porosity and *EWC* values slightly increased with an increase in Al_2O_3 content according to Arsuaga et al. (2013) [45], even though average pore radius was barely affected by adding Al_2O_3 [53]. Therefore, the values of membrane porosity

and EWC increased when additive concentration was higher due to the increment of the number of pores in the membrane surface and/or the pore size of the existing pores. Also, it can be observed that an increase of polymer concentration in the casting solution led to a membrane with low porosity and pore size in comparison with lower polymer concentrations [54].

3.5 Contact angle measurement

Water contact angle is also an important parameter in measuring of the surface hydrophilicity. The contact angle measurements were done for membranes with the best behaviour in terms of rejection, membrane porosity and *EWC*. These membranes were membranes based on PES. Contact angle measurement is very important to evaluate the hydrophilicity of modified membranes because the hydrophobic nature of PES causes an excessive fouling tendency [55]. Table 3 shows the results obtained for all the PES membranes with and without additives. PES membranes without an additive (PES1 and PES4) had similar contact angle than those obtained for non-porous PES film (about 76º) by other researchers [11]. These researchers demonstrated that the value of the contact angle is influenced by membrane material as well as by membrane surface porosity. This could be the reason of the fluctuation in the contact angle results for the same material. As clearly seen in Table 3, membranes prepared with hydrophilic additive showed lower contact angle than the unmodified membranes. This could be explained because modified membranes had higher surface porosity (see Table 2). Thus, as the membrane contact angle decreased, membrane surface hydrophilicity increased [23,27]. An increase in Al_2O_3 concentration caused a decrease in the contact angle [53,54], due to its higher affinity for water than base polymer. The same trend was observed for a high PEG 400 content. Due to the hydrophilic nature of PEG, the PEG

segments in the base polymer during the immersion precipitation process can diffuse preferentially on the membrane surface, causing an improvement of wettability on the membrane surface. Therefore, contact angle is closely related with surface energy [56]. The incorporation of both additives caused a higher decrease in the contact angle than the addition of Al_2O_3, indicating that the PES membranes with PEG/Al_2O_3 as additive (PES3, PES4, PES7 and PES8) were the most hydrophilic membrane. These results demonstrated that the membrane hydrophilicity increased with the combination of both additives.

3.6 Energy dispersive X-ray (EDX) analysis

EDX analysis was performed to obtain the element composition of membrane surface. The results in the top layer are shown in Table 4. EDX analysis demonstrated the presence of C, O, S for all the membranes, including Al for all the modified membranes. As Ma et al. (2009) demonstrated, oxygen was present in all the selected regions of the membranes, even in the unmodified membrane [57]. Therefore, the identification of all possible chemical states of oxygen is difficult. Al element was incorporated and distributed homogeneously through the top layer after the coating process as Al_2O_3. The presence of Al was somewhat higher in PES membranes modified only with Al_2O_3 (PES2 and PES5) than in PES membranes with PEG/Al_2O_3 as additive (PES3, PES4, PES5 and PES6), because macrovoids formation caused by the addition of PEG reoriented the Al_2O_3 nanoparticles in the membrane, diminishing its presence. However, there was no a great difference between the values obtained by EDX analysis for Al_2O_3 in all the modified membranes. Furthermore, it can be found that the content of sulphur on the surface of the unmodified membrane was higher than membranes with additive, because its presence decreased by the incorporation of higher amounts of additives.

3.7 Morphological studies

AFM analyses were performed to investigate the surface morphology at a nanoscopic scale and quantify the surface roughness of a membrane. Table 3 indicates the roughness values of the different membrane surfaces in terms of the average roughness (S_a) and the root mean square roughness (S_q). AFM results showed that S_a value of PES1 was 3.09 nm. When PES concentration in the membrane increased (PES5), membrane surface became slightly smoother, achieving a roughness value of 2.75 nm. This phenomenon may be due to the decrease in pore size caused by the increment in the number of polymer molecules in the membrane surface. As Rahimpour et al. (2009) demonstrated, a direct correlation between surface roughness and membrane wettability exists when the base polymer of the membrane surface is identical. Consequently, membrane with higher hydrophilicity has lower surface roughness and vice-versa [55].

Comparing the values obtained at the same PES concentration, the surface roughness of PES/Al_2O_3 membranes was scarcely higher than the unmodified PES membranes. So, Al_2O_3 content did not significantly affect the roughness of the PES membrane and thus, their mean pore size and membrane porosity had similar values (see Section 3.4). The small improvement of membrane roughness may be attributed to the surface enrichment of Al_2O_3 nanoparticles. Generally, high surface roughness allows more adhesion of the foulants on the membrane surface [33]. However, this typical behaviour changes when additives with hydrophilic nature are incorporated in the polymer structure. As Al_2O_3 nanoparticles were porous and ceramic, the increase in roughness caused by the accumulation of hydrophilic Al_2O_3 nanoparticles on the membrane surface significantly

564 improved the membrane surface hydrophilicity, which reduced the interaction between
565 foulants and membrane surface [53].
566
567 In addition, S_a improved with increasing the PEG content into the casting solution,
568 which was remarkable for membranes with a low PES concentration. This indicated that
569 the PEG chains tended to aggregate on the porous membrane surface, which endows the
570 PES membrane with a more porous and relatively rougher surface. These results are in
571 good agreement with those obtained by Idris et al. (2007). At 20 wt% PES
572 concentration, these authors demonstrated that the addition of PEG of different
573 molecular weight barely affected the roughness parameter. However, the surface
574 roughness slightly increased when PEG 400 was added [17].
575
576 Thus, these results showed that higher surface roughness caused by the presence of
577 hydrophilic additives in the membrane was related to higher porosity as well as lower
578 water contact angle of the membrane, which led to an improvement in hydrophilicity
579 and thus, in the antifouling properties [38,53]. Therefore, these results confirmed the
580 enhancement in hydrophilicity of the membrane surface and pore walls with the
581 introduction of PEG/Al_2O_3 nanoparticles.
582
583 Microscopic study through SEM analysis was carried out to have qualitative
584 information about surface and cross-sectional morphology of all the prepared
585 membranes. This technique is suitable for microscopic observations of the membrane
586 morphology. The effect of the presence of different additives is shown in the Fig. 7. The
587 unmodified membrane had an asymmetric structure consisting of a dense thin top layer,
588 a porous finger-like substructure, and nonwoven support (see Fig. 7 (A and D)). The

589 formation of this typical structure and its inherent phenomena had been explained by
590 previous researchers [58-60]. As it can be seen in Fig. 7 (B and E), PES/Al_2O_3
591 membrane had a similar structure to that of the unmodified membranes. However, the
592 incorporation of Al_2O_3 caused the formation of nano-sized pores, which were uniformly
593 dispersed along the entire membrane. The sublayer changed to a denser sponge-like
594 structure, making a more hydrophilic membrane by the suppression in formation of
595 macrovoids and the enhancement in formation of micropores without changing the
596 asymmetric nature of these membranes [27,61]. As it can be observed, in turn, there
597 were some Al_2O_3 nanoparticles along the membrane structure, close to the formed
598 nanopores above mentioned. Also, some agglomerations of Al_2O_3 nanoparticles can be
599 seen in this membrane. These agglomerations could cause the blockage of some pores
600 along the membrane structure and could lead to a low value of average pore radius [23].
601
602 Finally, the presence of such nanoparticles in the membrane structure and formed
603 agglomerations can be also observed in Fig. 7 (C and F). The addition of PEG
604 transformed the finger-like cavities in the substructure into a macrovoids structure due
605 to the rapid formation of the membrane (known as instantaneous demixing) in the
606 coagulation bath, which increases the membrane thickness and enhances the macrovoid
607 formation in the sublayer [20]. Therefore, the membrane pore size as well as the
608 membrane hydrophilicity increased with this new formed substructure and then, the
609 hydraulic permeability also increased and the solute rejection and the fouling resistance
610 decreased [20,62].
611
612 **4. CONCLUSIONS**

The characteristics and performance of three different polymeric membranes (PES, PS and PEI) prepared with two hydrophilic nano-sized additives (PEG and Al_2O_3) have been investigated. All the prepared membranes were synthesized by phase-inversion process, showing similar MWCO (30 kDa). When polymer concentration decreased, hydraulic permeability increased and then, membrane resistance decreased. The same trend was caused by the incorporation of additives in the casting solution. In terms of solute rejection, when the polymer concentration increased, pore size decreased as well as the MWCO. PES membranes presented the best solute rejection among the membranes prepared, where PES membranes prepared with Al_2O_3 as additive showed the highest solute rejection using different molecular weights of PEG.

Incorporation of PEG/Al_2O_3 resulted in a more hydrophilic membrane, showing better results in terms of contact angle, surface roughness, membrane porosity and *EWC*. However, the combined addition of PEG/Al_2O_3 enhanced membrane hydrophilicity with the formation of macrovoids, which negatively affected to antifouling properties when PEG 400 content was higher than 2 wt%. Furthermore, the average pore radius of membranes increased with the presence of PEG, whereas this parameter was barely affected by adding Al_2O_3. According to fouling tests, incorporation of PEG/Al_2O_3 resulted in a more hydrophilic membrane with a higher normalized flux ratio, reducing the hydrophobic interaction between the membrane surface and foulants. These results indicated that the addition of PEG/Al_2O_3 improved the antifouling properties of PES membranes when PEG 400 is added in appropriate amounts, modifying the membrane morphology to a sponge-like substructure.

5. ACKNOWLEDGEMENTS

638 The authors of this work thank the financial support of CDTI (Centre for Industrial
639 Technological Development) depending on the Spanish Ministry of Science and
640 Innovation. The authors also thank the Center for Biomaterials and Tissue Engineering
641 (Universitat Politècnica de València) for contact angle measurements and BASF
642 (Germany) and General Electric (United States) for supplying the polymers used.
643

644 ## 6. REFERENCES AND NOTES

645 [1] R.W. Baker. Membrane Technology and Applications, second ed., John Wiley &
646 Sons Ltd., Chichester, 2004.
647 [2] S. Barredo-Damas, M.I. Alcaina-Miranda, M.I. Iborra-Clar, J.A. Mendoza-Roca,
648 Application of tubular ceramic ultrafiltration membranes for the treatment of integrated
649 textile wastewaters, Chem. Eng. J. 192 (2012) 211-218.
650 [3] Y. Zhang, Z. Jin, X. Shan, J. Sunarso, P. Cui, Preparation and characterization of
651 phosphorylated Zr-doped hybrid silica/PSf composite membrane, J. Hazard. Mater. 186
652 (2011) 390-395.
653 [4] W. Zhao, Q. Mou, X. Zhang, J. Shi, S. Sun, C. Zhao, Preparation and
654 characterization of sulfonated polyethersulfone membranes by a facile approach, Eur.
655 Polym. J. 49 (2013) 738-751.
656 [5] M.K. Sinha, M.K. Purkait, Increase in hydrophilicity of polysulfone membrane
657 using polyethylene glycol methyl ether, J. Membr. Sci. 437 (2013) 7-16.
658 [6] V. Vatanpour, S.S. Madaeni, R. Moradian, S. Zinadini, B. Astinchap, Novel
659 antifouling nanofiltration polyethersulfone membrane fabricated from embedding TiO_2
660 coated multiwalled carbon nanotubes, Sep. Purif. Technol. 90 (2012) 69-82.

[7] M-J. Corbatón-Báguena, M-C. Vincent-Vela, S. Álvarez-Blanco, J. Lora-García, Analysis of two ultrafiltration fouling models and estimation of model parameters as a function of operational conditions, Transp. Porous Med. 99 (2013)

[8] Y. Su, C. Li, W. Zhao, Q. Shi, H. Wang, Z. Jiang, S. Zhu, Modification of polyethersulfone ultrafiltration membranes with phosphorylcholine copolymer can remarkably improve the antifouling and permeation properties, J. Membr. Sci. 322 (2008) 171-177.

[9] Y.S. Li, L. Yan, C.B. Xiang, L.J. Hong, Treatment of oily wastewater by organic-inorganic composite tubular ultrafiltration (UF) membranes, Desalination 196 (2006) 76-83.

[10] A.L. Ahmad, A.A. Abdulkarim, B.S. Ooi, S. Ismail, Recent development in additives modifications of polyethersulfone membrane for flux enhancement, Chem. Eng. J. 223 (2013) 246-267.

[11] H. Susanto, M. Ulbricht, Photografted thin polymer hydrogel layers on PES ultrafiltration membranes: characterization, stability, and influence on separation performance, Langmuir 23 (2007) 7818-7830.

[12] H. Susanto, M. Ulbricht, Characteristics, performance and stability of polyethersulfone ultrafiltration membranes prepared by phase separation method using different macromolecular additives, J. Membr. Sci. 327 (2009) 125-135.

[13] A. Razmjou, J. Mansouri. V. Chen, The effects of mechanical and chemical modification of TiO_2 nanoparticles on the surface chemistry, structure and fouling performance of PES ultrafiltration membranes, J. Membr. Sci. 378 (2011) 73-84.

[14] A. Sotto, A. Boromand, R. Zhang, P. Luis, J.M. Arsuaga, J. Kim, B. Van der Bruggen, Effect of nanoparticle aggregation at low concentrations of TiO_2 on the

685 hydrophilicity, morphology, and fouling resistance of PES-TiO_2 membranes, J. Colloid
686 Interf. Sci. 363 (2011) 540-550.
687 [15] T.A. Saleh, V.K. Gupta, Synthesis and characterization of alumina nano-particles
688 polyamide membrane with enhanced flux rejection performance, Sep. Purif. Technol. 89
689 (2012) 245-251.
690 [16] Y. Liu, G.H. Koops, H. Strathmann, Characterization of morphology controlled
691 polyethersulfone hollow fiber membranes by the addition of polyethylene glycol to the
692 dope and bore liquid solution, J. Membr. Sci. 223 (2003) 187-199.
693 [17] A. Idris, N. M. Zain, M.Y. Noordin, Synthesis, characterization and performance of
694 asymmetric polyethersulfone (PES) ultrafiltration membranes with polyethylene glycol
695 of different molecular weights as additives, Desalination 207 (2007) 324-339.
696 [18] S. Qiu, L.G. Wu, X.J. Pan, L. Zhang, H.L. Chen, C.J. Gao, Preparation and
697 properties of functionalized carbon nanotube/PSF blend ultrafiltration membranes, J.
698 Membr. Sci. 342 (2009) 165-172.
699 [19] S.A. Al Malek, M.N. Abu Seman, D. Johnson, N. Hilal, Formation and
700 characterization of polyethersulfone membranes using different concentrations of
701 polyvinylpyrrolidone, Desalination 288 (2012) 31-39.
702 [20] E. Saljoughi, M. Amirilargani, T. Mohammadi, Effect of PEG additive and
703 coagulation bath temperature on the morphology, permeability and thermal/chemical
704 stability of asymmetric CA membranes, Desalination 262 (2010) 72-78.
705 [21] Q. Shi, Y. Su, W. Zhao, C. Li, Y. Hu, Z. Jiang, S. Zhu, Zwitterionic
706 polyethersulfone ultrafiltration membrane with superior antifouling property, J. Membr.
707 Sci. 319 (2008) 271-278.

708 [22] A. Rahimpour, S.S. Madaeni, Improvement of performance and surface properties
709 of nano-porous polyethersulfone (PES) membrane using hydrophilic monomers as
710 additives in the casting solution, J. Membr. Sci. 360 (2010) 371-379.
711 [23] E. Yuliwati, A.F. Ismail, T. Matsuura, M.A. Kassim, M.S. Abdullah, Effect of
712 modified PVDF hollow fiber submerged ultrafiltration membrane for refinery
713 wastewater treatment, Desalination 283 (2011) 214-220.
714 [24] X-M. Wang, X-Y. Li, K. Shih, In situ embedment and growth of anhydrous and
715 hydrated aluminium oxide particles on polyvinylidene fluoride (PVDF) membranes, J.
716 Membr. Sci. 368 (2011) 134-143.
717 [25] S. Balta, A. Sotto, P. Luis, I. Benea, B. Van der Bruggen, J. Kim, A new outlook
718 on membrane enhancement with nanoparticles: the alternative of ZnO, J. Membr. Sci.
719 389 (2012) 155-161.
720 [26] N.A. Ochoa, M. Masuelli, J. Marchese, Effect of hydrophilicity on fouling of an
721 emulsified oil wastewater with PVDF/PMMA membranes, J. Membr. Sci. 226 (2003)
722 203-211.
723 [27] L. Yan, Y.S. Li, C.B. Xiang, Preparation of poly(vinylidene fluoride) (PVDF)
724 ultrafiltration membrane modified by nano-sized alumina (Al_2O_3) and its antifouling
725 research, Polymer 46 (2005) 7701-7706.
726 [28] B. Chakrabarty, A.K. Ghoshal, M.K. Purkait, Effect of molecular weight of PEG
727 on membrane morphology and transport properties, J. Membr. Sci. 309 (2008) 209-221.
728 [29] C.D. Jones, M. Fidalgo, M.R. Wiesner, A.R. Barron, Alumina ultrafiltration
729 membranes derived from carboxylate aluminoxane nanoparticles, J. Membr. Sci. 193
730 (2001) 175-184.

731 [30] F. Liu, M.R. Moghareh Abed, K. Li, Preparation and characterization of
732 poly(vinylidene fluoride) (PVDF) based ultrafiltration membranes using nano γ-Al_2O_3,
733 J. Membr. Sci. 366 (2011) 97-103.
734 [31] L. Shieh, T.S. Chung, R. Wang, M.P. Srinivasan, D.R. Paul, Gas separation
735 performance of poly(4-vinylpiridine)/polyetherimide composite hollow fibers, J.
736 Membr. Sci. 182 (2001) 111-123.
737 [32] M. Liu, Y-M. Wei, Z-L. Xu, R-Q. Guo, L-B. Zhao, Preparation and
738 characterization of polyethersulfone microporous membrane via thermally induced
739 phase separation with low critical solution temperature system, J. Membr. Sci. 437
740 (2013) 169-178.
741 [33] P. Daraei, S.S. Madaeni, N. Ghaemi, M.A. Khadivi, B. Astinchap, R. Moradian,
742 Fouling resistant mixed matrix polyethersulfone membranes blended with magnetic
743 nanoparticles: Study of magnetic field induced casting, Sep. Purif. Technol. 109 (2013)
744 111-121.
745 [34] C. Barth, M.C. Gonçalves, A.T.N. Pires, J. Roeder, B.A. Wolf, Asymmetric
746 polysulfone and polyethersulfone membranes: effects of thermodynamic conditions
747 during formation on their performance, J. Membr. Sci. 169 (2000) 287-299.
748 [35] G. Wu, S. Gan, L. Cui, Y. Xu, Preparation and characterization of PES/TiO2
749 composite membranes, Appl. Sur. Sci. 254 (2008) 7080-7086.
750 [36] N. Maximous, G. Nakhla, W. Wan, K. Wong, Performance of a novel ZrO_2/PES
751 membrane for wastewater filtration, J. Membr. Sci. 352 (2010) 222-230.
752 [37] Y. Kim, D. Rana, T. Matsuura, W-J. Chung, Influence of surface modifying
753 macromolecules on the surface properties of poly(ether sulfone) ultra-filtration
754 membranes, J. Membr. Sci. 338 (2009) 84-91.

755 [38] A. Ananth, G. Arthanareeswaran, H. Wang, The influence of tetraethylorthosilicate
756 and polyethyleneimine on the performance of polyethersulfone membranes,
757 Desalination 287 (2012) 61-70.
758 [39] W. Yoshida, Y. Cohen, Topological AFM characterization of graft polymerized
759 silica membranes, J. Membr. Sci. 215 (2003) 249-264.
760 [40] Y Li, H. Zhang, H. Zhang, J. Cao, W. Xu, X. Li, Hydrophilic porous poly(sulfone)
761 membranes modified by UV-initiated polymerization for vanadium flow battery
762 application, J. Membr. Sci. 454 (2014) 478-487.
763 [41] N. Maximous, G. Nakhla, W. Wan, K. Wong, Preparation, characterization and
764 performance of Al_2O_3/PES membrane for wastewater filtration, J. Membr. Sci. 341
765 (2009) 67-75.
766 [42] H. Lohokare, Y. Bhole, S. Taralkar, U. Kharul, Poly(acrylonitrile) based
767 ultrafiltration membranes: Optimization of preparation parameters, Desalination 282
768 (2011) 46-53.
769 [43] I.C. Kim, K.H. Lee, T.M. Tak, Preparation and characterization of integrally
770 skinned uncharged polyetherimide asymmetric nanofiltration membrane, J. Membr. Sci.
771 183 (2001) 235-247.
772 [44] N. Maximous, G. Nakhla, K. Wong, W. Wan, Optimization of Al_2O_3/PES
773 membranes for wastewater filtration, Sep. Purif. Technol. 73 (2010) 294-301.
774 [45] J.M. Arsuaga, A. Sotto, G. del Rosario, A. Martínez, S. Molina, S.B. Teli, J. de
775 Abajo, Influence of the type, size, and distribution of metal oxide particles on the
776 properties of nanocomposite ultrafiltration membranes, J. Membr. Sci. 428 (2013) 131-
777 141.
778 [46] J-H. Kim, K-H. Lee, Effect of PEG additive on membrane formation by phase
779 inversion, J. Membr. Sci. 138 (1998) 153-163.

780 [47] S. Platt, M. Mauramo, S. Butylina, M. Nyström, Retention of PEGs in cross-flow
781 ultrafiltration through membranes, Desalination 149 (2002) 417-422.
782 [48] M. Sivakumar, D.R. Mohan, R. Rangarajan, Studies on cellulose acetate-
783 polysulfone ultrafiltration membranes II. Effect of additive concentration, J. Membr.
784 Sci. 268 (2006) 208-219.
785 [49] K. Kimmerle, H. Strathmann, Analysis of the structure-determining process of
786 phase inversion membranes, Desalination 79 (1990) 283-302.
787 [50] Y. Ma, F. Shi, J. Ma, M. Wu, J. Zhang, C. Gao, Effect of PEG additive on the
788 morphology and performance of polysulfone ultrafiltration membranes, Desalination
789 272 (2011) 51-58.
790 [51] C. Feng, R. Wang, B. Shi, G. Li, Y. Wu, Factors affecting pore structure and
791 performance of poly(vinylidene fluoride-co-hexafluoro propylene) asymmetric porous
792 membrane, J. Membr. Sci. 277 (2006) 55-64.
793 [52] A. Jayalakshmi, S. Rajesh, S. Senthilkumar, D. Mohan, Epoxy functionalized
794 poly(ether-sulfone) incorporated cellulose acetate ultrafiltration membrane for the
795 removal of chromium ions, Sep. Purif. Technol. 90 (2012) 120-132.
796 [53] L. Yan, Y.S. Li, C.B. Xiang, S. Xiandia, Effect of nano-sized Al_2O_3-particle
797 addition on PVDF ultrafiltration membrane performance, J. Membr. Sci. 276 (2006)
798 162-167.
799 [54] B.S. Lalia, V. Kochkodan, R. Hashaikeh, N. Hilal, A review on membrane
800 fabrication: structure, properties and performance relationship, Desalination 326 (2013)
801 77-95.
802 [55] A. Rahimpour, S.S. Madaeni, M. Jahanshahi, Y. Mansourpanah, N. Mortazavian,
803 Development of high performance nano-porous polyethersulfone ultrafiltration

804 membranes with hydrophilic surface and superior antifouling properties, Appl. Sur. Sci.
805 255 (2009) 9166-9173.
806 [56] Y.H. Cho, H.W. Kim, S.Y. Nam, H.B. Park, Fouling-tolerant polysulfone-
807 poly/ethylene oxide) random copolymer ultrafiltration membranes, J. Membr. Sci. 379
808 (2011) 296-306.
809 [57] J. Ma, Z. Wang, M. Pan, Y. Guo, A study on the multifunction of ferrous chloride
810 in the formation of poly(vinylidene fluoride) ultrafiltration membranes, J. Membr. Sci.
811 341 (2009) 214-224.
812 [58] C.A. Smolders, A.J. Reuvers, R.M. Boom, I.M. Wienk, Microstructures in phase-
813 inversion membranes. Part 1. Formation of macrovoids, J. Membr. Sci. 73 (1992) 259-
814 275.
815 [59] R.M. Boom, I.M. Wienk, Th. Van den Boomgaard, C.A. Smolders,
816 Microstructures in phase inversion membranes. Part 2. The role of a polymeric additive,
817 J. Membr. Sci. 73 (1992) 277-292.
818 [60] I.M. Wienk, R.M. Boom, M.A.M. Beerlage, A.M.W. Bulte, C.A. Smolders, H.
819 Strathmann, Recent advances in the formation of phase inversion membranes made
820 from amorphous or semi-crystalline polymers, J. Membr. Sci. 113 (1996) 361-371.
821 [61] A.T.T. Tran, D.A. Patterson, B.J. James, Investigating the fasibility of using
822 polysulfone-montmorillonite composite membranes for protein adsorption, J. Food Eng.
823 112 (2012) 38-49.
824 [62] S. Wongchitphimon, R. Wang, R. Jiraratananon, L. Shi, C. H. Loh, Effect of
825 polyethylene glycol (PEG) as an additive on the fabrication of polyvinylidene fluoride-
826 co-hexafluropropylene (PVDF-HFP) asymmetric microporous hollow fiber membranes,
827 J. Membr. Sci. 369 (2011) 329-338.
828

7. LIST OF SYMBOLS

Variables

A_m	Effective area of the membrane (m^2)
C_A	Concentration of PEG in feed stream (wt%)
C_P	Concentration of PEG in permeate stream (wt%)
J	Steady-state permeate flux (L m^{-2} h^{-1})
J_f	Permeate flux during PEG ultrafiltration (L m^{-2} h^{-1})
J_{f1}	Permeate flux of the membranes obtained at the beginning of each fouling cycle (L m^{-2} h^{-1})
J_{f2}	Permeate flux of the membranes after the fouling process (L m^{-2} h^{-1})
J_p	Permeate flux (L m^{-2} h^{-1})
J_W	Permeate water flux of the tested membranes (L m^{-2} h^{-1})
M_W	Molecular weight (Da)
N	Number of points within the given area (dimensionless)
NFR	Normalized flux ratio (%)
P_h	Hydraulic permeability (L m^{-2} h^{-1} MPa^{-1})
Q_W	Water flow (m^3 s^{-1})
r_m	Average pore radius (m)
R	Solute rejection (%)
R_m	Membrane resistance (m^{-1})
S_a	Average roughness (nm)
S_q	Root mean square roughness (nm)
t	Experimental time interval (h)
T	Feed temperature (°C)
V	Total volume permeated during an experimental time interval (L)

W_D	Weight of dry membranes (g)
W_W	Weight of wet membranes (g)
Z	Height values of the surface sample (nm)
Z_{avg}	Average of the Z values of the sample (nm)
Z_i	Z value currently measured (nm)
ΔP	Transmembrane pressure (MPa)

Greek letters

ε	Membrane porosity (%)
ζ	membrane thickness (m)
μ	Dynamic water viscosity (Pa s)
ρ_p	Density of the polymer (g cm^{-3})
ρ_W	Density of pure water at operating conditions (g cm^{-3})

Abbreviations

AFM	Atomic force microscopy
BSA	Bovine serum albumin
CA	Cellulose acetate
CBT	Coagulation bath temperature
DMA	N,N-Dimethylacetamide
EDX	Energy dispersive X-ray
EWC	Equilibrium water content
MWCO	Molecular weight cut-off
PAN	Polyacrylonitrile
PE	Polyethylene

879	PEG	Polyethyleneglycol
880	PEI	Polyetherimide
881	PES	Polyethersulfone
882	PMMA	Polymethyl methacrylate
883	PP	Polypropylene
884	PS	Polysulfone
885	PVDF	Polyvinylidene fluoride
886	PWF	Pure water flux
887	SEM	Scanning electron microscopy
888	UF	Ultrafiltration

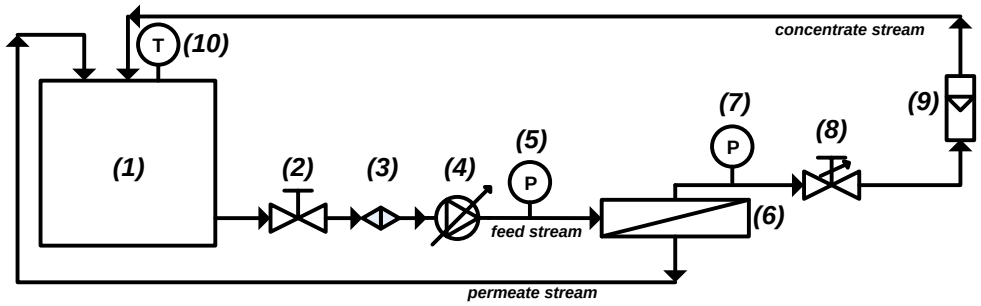

Fig. 1. Schematic diagram of experimental UF setup: (1) temperature-controlled feed tank, (2) feed valve, (3) pre-filter, (4) centrifugal pump, (5) manometer, (6) membrane module, (7) manometer; (8) valve, (9) flow meter, (10) thermometer.

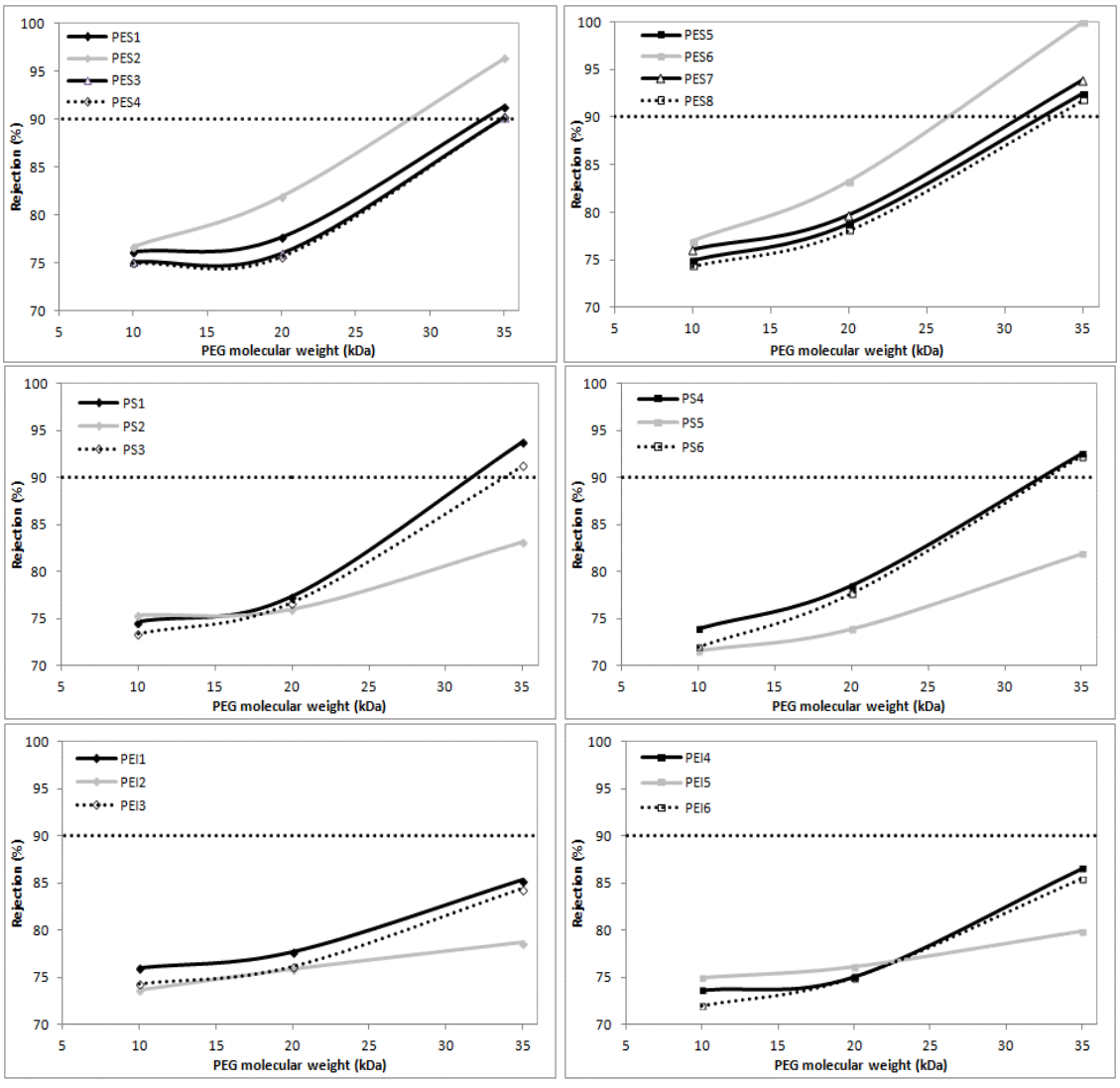

Fig. 2. Experimental solute rejection as a function of PEG molecular weight for different polymeric membranes, where dotted line represents the molecular weight cut-off (MWCO). Experimental conditions were: 25 ºC, 2.08 m s^{-1}, ΔP ranging from 50 to 400 kPa.

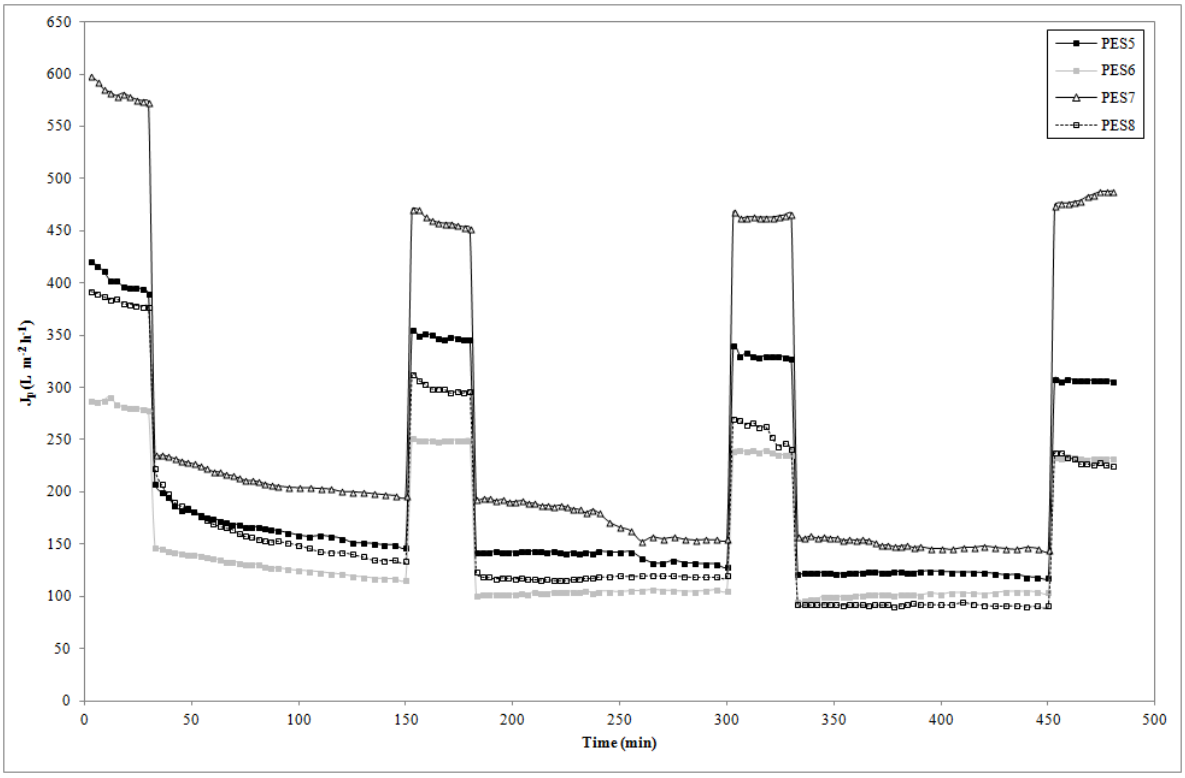

Fig. 3. Permeate flux versus filtration time for PES membranes with a polymer concentration of 20 wt%, with and without additive during one PWF test and three PEG fouling/rinsing cycles (25 ºC, 200 kPa, 2.08 m s^{-1}).

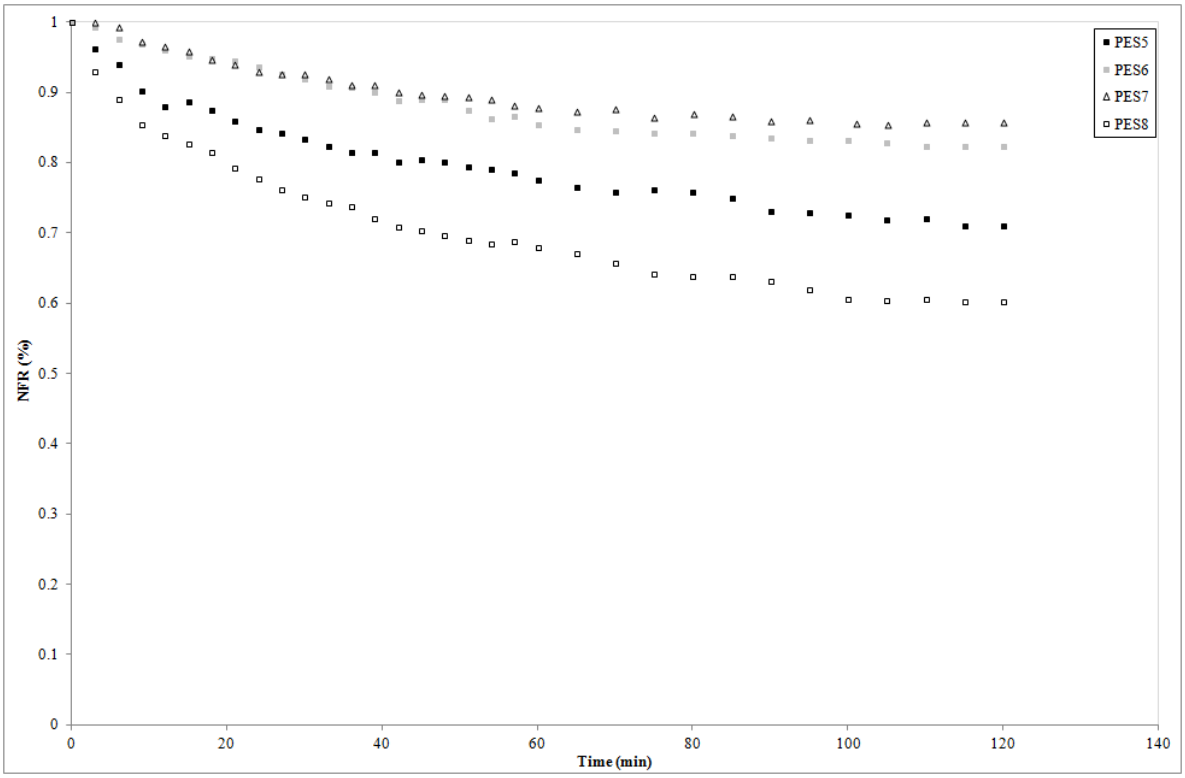

Fig. 4. Normalized flux ratio (NFR) in PEG ultrafiltration of PES membranes with a polymer concentration of 20 wt%, with and without additive (25 ºC, 200 kPa, 2.08 m s^{-1}).

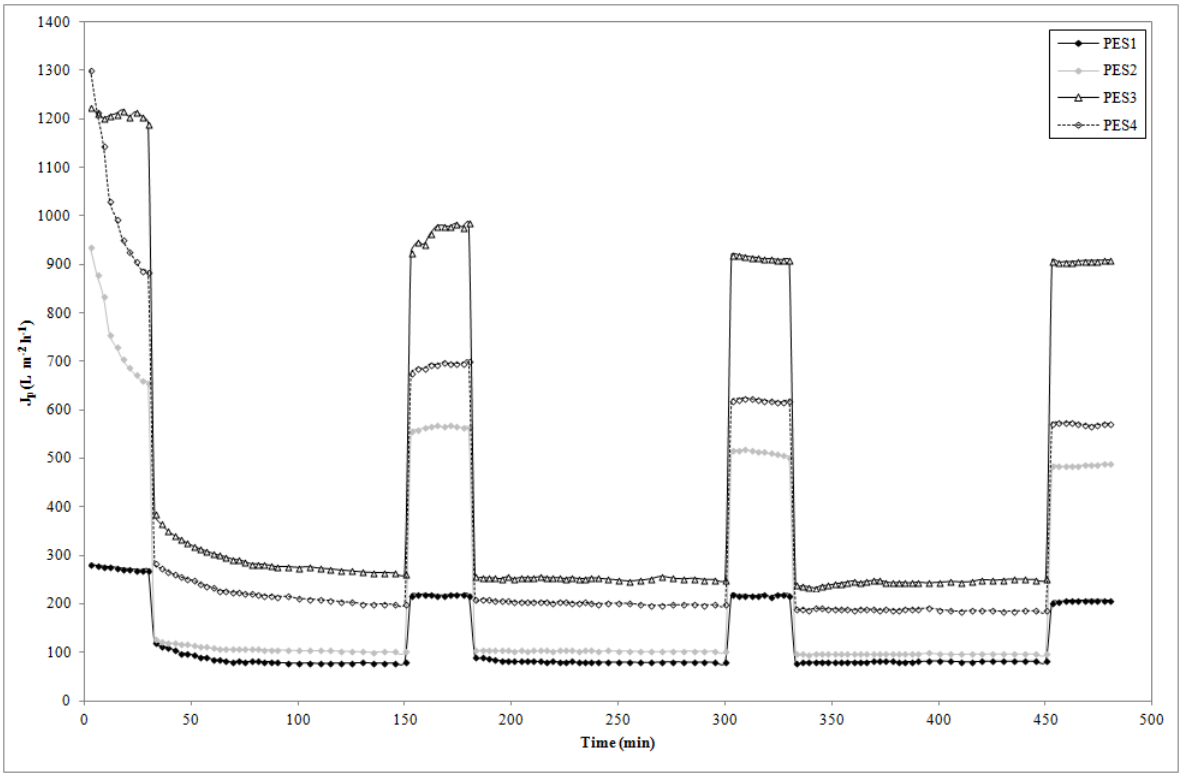

Fig. 5. Permeate flux versus filtration time for PES membranes with a polymer concentration of 15 wt%, with and without additive during one PWF test and three PEG fouling/rinsing cycles (25 ºC, 200 kPa, 2.08 m s^{-1}).

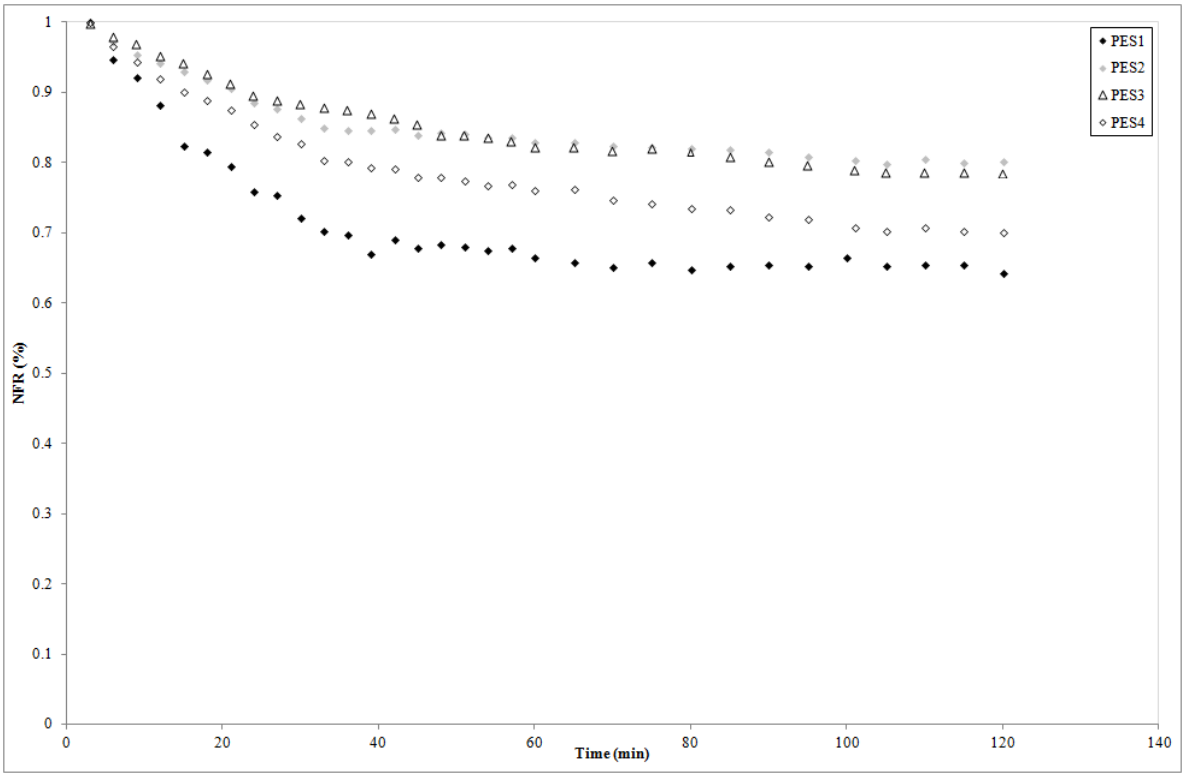

Fig. 6. Normalized flux ratio (NFR) in PEG ultrafiltration of PES membranes with a polymer concentration of 15 wt%, with and without additive (25 ºC, 200 kPa, 2.08 m s^{-1}).

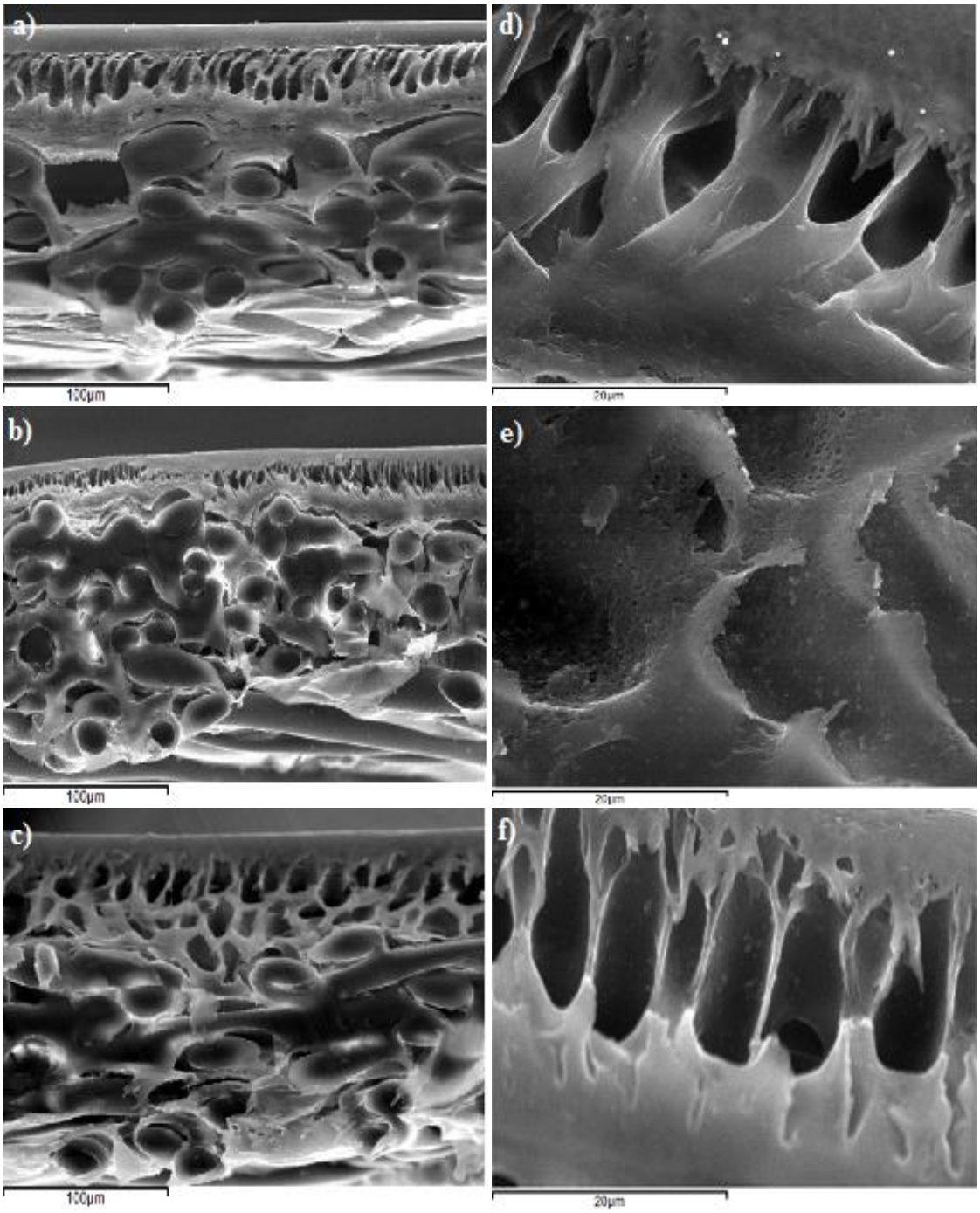

Fig. 7. SEM images of the cross-section morphology of prepared membranes. From the top to the bottom panel: unmodified PES (A and D), PES modified with Al_2O_3 (B and E), and PES membrane modified with PEG/Al_2O_3 (C and F), respectively.

Table 1. Membrane composition and hydraulic characteristics for all prepared polymeric membranes

Membrane	Composition of casting solution (wt%)				Hydraulic permeability	Membrane resistance $\cdot 10^{-11}$
	P	DMA	Al_2O_3	PEG	(L m^{-2} h^{-1} kPa^{-1})	(m^{-1})
PES1	15	85	---	---	4.998	8.060
PES2	15	84.5	0.5	---	7.828	5.146
PES3	15	82.5	0.5	2.0	9.422	4.275
PES4	15	80	0.5	4.5	9.601	4.196
PES5	20	80	---	---	2.352	17.017
PES6	20	79.5	0.5	---	2.612	15.422
PES7	20	77.5	0.5	2.0	4.210	9.567
PES8	20	75	0.5	4.5	5.146	7.828
PS1	15	85	---	---	11.828	3.406
PS2	15	84.5	0.5	---	14.696	2.741
PS3	15	80	0.5	4.5	15.408	2.614
PS4	20	80	---	---	4.658	8.648
PS5	20	79.5	0.5	---	5.102	7.895
PS6	20	75	0.5	4.5	5.742	7.015
PEI1	15	85	---	---	10.591	3.803
PEI2	15	84.5	0.5	---	28.011	1.438
PEI3	15	80	0.5	4.5	32.001	1.259
PEI4	20	80	---	---	10.410	3.870
PEI5	20	79.5	0.5	---	11.770	3.422
PEI6	20	75	0.5	4.5	16.194	2.487

P, polymer; Membrane area = 100 cm^2; Temperature = 25 ºC; Coagulation Bath Temperature (CBT) = 18 ºC.

Table 2. Properties of all prepared flat membranes in terms of membrane porosity (ε), equilibrium water content (EWC) and average pore radius (r_m)

Membrane	ε (%)	EWC (%)	r_m (nm)
PES1	71.75	70.44	21.04
PES2	75.41	75.20	20.53
PES3	78.76	79.77	21.92
PES4	83.07	83.52	25.57
PES5	69.11	68.52	14.32
PES6	73.82	71.69	12.21
PES7	81.17	81.27	17.54
PES8	86.55	86.25	17.85

Table 3. Water contact angles measured by sessile drop method and roughness parameters for PES membranes unmodified and modified with different additives

Membrane	Contact Angle (º)	Surface roughness (nm)	
		S_a	S_q
PES1	75.9±1.1	3.09	3.93
PES2	69.6±2.8	3.42	4.64
PES3	56.9±2.4	5.54	7.04
PES4	58.2±2.6	5.46	6.96
PES5	72.9±1.5	2.75	3.52
PES6	65.3±2.0	2.98	3.76
PES7	57.2±2.7	3.60	4.63
PES8	57.6±2.9	3.27	4.37

Table 4. EDX results for PES membranes modified with different additives

Sample	Element							
	C K		S K		O K		Al K	
	wt%	at%	wt%	at%	wt%	at%	wt%	at%
PES1	23.58	29.88	5.52	2.62	70.90	67.50	0.00	0.00
PES2	23.20	29.52	5.48	2.61	70.63	67.47	0.69	0.39
PES3	23.29	29.61	5.41	2.57	70.69	67.47	0.62	0.35
PES4	23.55	29.86	5.11	2.43	70.83	67.43	0.51	0.28
PES5	23.20	29.52	6.00	2.86	70.80	67.62	0.00	0.00
PES6	23.29	29.61	5.53	2.63	70.59	67.43	0.59	0.33
PES7	23.59	29.90	4.98	2.36	70.89	67.44	0.54	0.30
PES8	24.31	30.59	4.06	1.91	71.18	67.24	0.45	0.26